# HLbL contribution to $(g-2)_\mu$ on the lattice

Christoph Lehner (BNL)

September 7, 2017 – FCCP2017

## **Collaborators** (RBC/UKQCD)

Tom Blum (Connecticut)
Norman Christ (Columbia)
Masashi Hayakawa (Nagoya)
Taku Izubuchi (BNL/RBRC)
**Luchang Jin (BNL $\rightarrow$ Connecticut)**
Christoph Lehner (BNL)
Chulwoo Jung (BNL)

# The anomalous magnetic moment

The anomalous magnetic moment $a$ can be expressed in terms of scattering of particle off a classical photon background

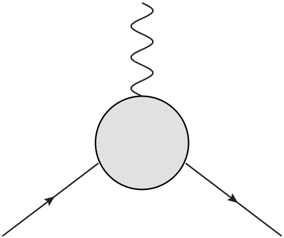

For external photon index $\mu$ with momentum $q$ the scattering amplitude can be generally written as

$$(-ie)\left[\gamma_\mu F_1(q^2) + \frac{i\sigma^{\mu\nu}q^\nu}{2m}F_2(q^2)\right]$$

with $F_2(0) = a$.

# Theory status – summary

| Contribution | Value $\times 10^{10}$ | Uncertainty $\times 10^{10}$ |
|---|---|---|
| QED (5 loops) | 11 658 471.895 | 0.008 |
| EW | 15.4 | 0.1 |
| **HVP LO** | 692.3 | **4.2** |
| HVP NLO | -9.84 | 0.06 |
| HVP NNLO | 1.24 | 0.01 |
| **Hadronic light-by-light** | 10.5 | **2.6** |
| Total SM prediction | 11 659 181.5 | 4.9 |
| BNL E821 result | 11 659 209.1 | 6.3 |
| FNAL E989/J-PARC E34 goal | | $\approx$ **1.6** |

A reduction of uncertainty for HVP and HLbL is needed. A systematically improvable first-principles calculation is desired.

# The Hadronic Light-by-Light contribution

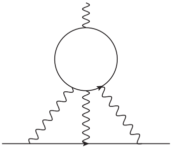

Quark-connected piece (charge factor of up/down quark contribution: $\frac{17}{81}$)

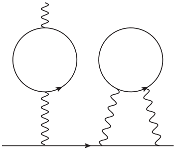

Dominant quark-disconnected piece (charge factor of up/down quark contribution: $\frac{25}{81}$)

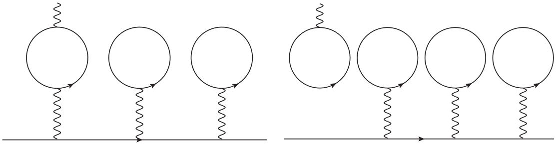

Sub-dominant quark-disconnected pieces (charge factors of up/down quark contribution: $\frac{5}{81}$ and $\frac{1}{81}$)

# Recent progress on the lattice – Overview

- $a_\mu^{\mathrm{HLbL}}$ in finite-volume QCD and QED:
  - PRD93(2016)014503 (RBC/UKQCD): Connected diagram with $m_\pi = 171$ MeV; $a_\mu^{\mathrm{HLbL}} = 13.21(68) \times 10^{-10}$
  - PRL118(2017)022005 (RBC/UKQCD): Connected and leading disconnected diagram with $m_\pi = 139$ MeV; $a_\mu^{\mathrm{HLbL}} = 5.35(1.35) \times 10^{-10}$ (potentially large finite-volume systematics)
- $a_\mu^{\mathrm{HLbL}}$ in finite-volume QCD and infinite-volume QED:
  - Method proposed and successfully tested against the lepton-loop analytic result: arXiv:1510.08384 (Mainz), arXiv:1609.08454 (Mainz)
  - Similar method plus subtraction scheme to reduce systematic errors; successfully tested against lepton-loop analytic result: PRD96(2017)034515 (RBC/UKQCD)
- The pion pole contribution to $a_\mu^{\mathrm{HLbL}}$:
  - PRD94(2016)074507 (Mainz): $a_{\mu;\mathrm{LMD+V}}^{\mathrm{HLbL};\pi^0} = 6.50(83) \times 10^{-10}$

T. Blum, N. Christ, M. Hayakawa, T. Izubuchi, L. Jin, and C.L., Phys. Rev. D 93, 014503 (2016)

Compute quark-connected contribution with new computational strategy

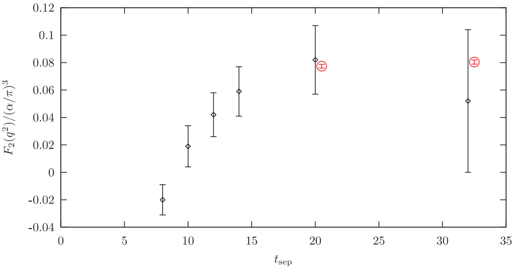


yields more than an order-of-magnitude improvement (red symbols) over previous method (black symbols) for a factor of $\approx 4$ smaller cost.

# New stochastic sampling method

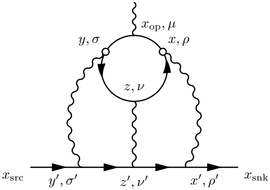


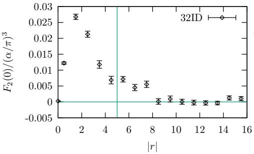


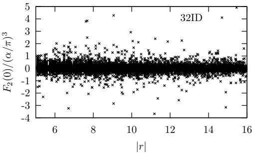


Stochastically evaluate the sum over vertices $x$ and $y$:

- Pick random point $x$ on lattice
- Sample all points $y$ up to a specific distance $r = |x - y|$, see vertical red line
- Pick $y$ following a distribution $P(|x - y|)$ that is peaked at short distances

## Cross-check against analytic result where quark loop is replaced by muon loop

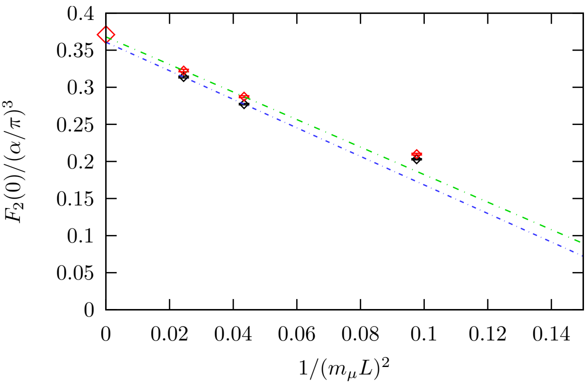


In Figure: $m_{\rm loop} = m_{\rm line}$

T. Blum, N. Christ, M. Hayakawa, T. Izubuchi, L. Jin, and C.L., PRL118(2017)022005

$$a_\mu^{\rm cHLbL} = \left.\frac{g_\mu - 2}{2}\right|_{\rm cHLbL} = (0.0926 \pm 0.0077)\left(\frac{\alpha}{\pi}\right)^3 = (11.60 \pm 0.96) \times 10^{-10} \quad (11)$$

$$a_\mu^{\rm dHLbL} = \left.\frac{g_\mu - 2}{2}\right|_{\rm dHLbL} = (-0.0498 \pm 0.0064)\left(\frac{\alpha}{\pi}\right)^3 = (-6.25 \pm 0.80) \times 10^{-10} \quad (12)$$

$$a_\mu^{\rm HLbL} = \left.\frac{g_\mu - 2}{2}\right|_{\rm HLbL} = (0.0427 \pm 0.0108)\left(\frac{\alpha}{\pi}\right)^3 = (5.35 \pm 1.35) \times 10^{-10} \quad (13)$$

Makes HLbL an unlikely candidate to explain the discrepancy!

Next need to address finite-volume and lattice-spacing systematics and sub-leading diagrams

Update on lattice-spacing systematics:

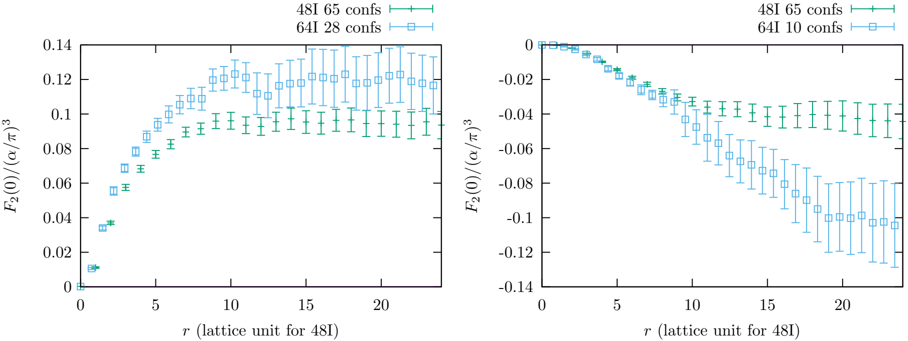


- Left: connected diagrams contribution. Right: leading disconnected diagrams contribution.
- $48^3 \times 96$ lattice, with $a^{-1} = 1.73\,\mathrm{GeV}$, $m_\pi = 139\,\mathrm{MeV}$, $m_\mu = 106\,\mathrm{MeV}$.
- $64^3 \times 128$ lattice, with $a^{-1} = 2.36\,\mathrm{GeV}$, $m_\pi = 135\,\mathrm{MeV}$, $m_\mu = 106\,\mathrm{MeV}$.

Waiting for more statistics on the fine lattice ensemble

# Finite-volume errors of the HLbL

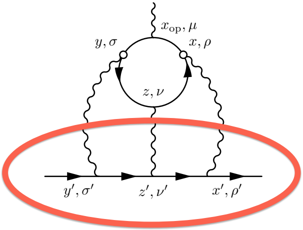


Remove power-law like finite-volume errors by computing the muon-photon part of the diagram in infinite volume (C.L. talk at lattice 2015 and Green et al. 2015, PRL115(2015)222003; Asmussen et al. 2016, PoS,LATTICE2016 164)

Now completed PRD96(2017)034515 with improved weighting function.

Details:

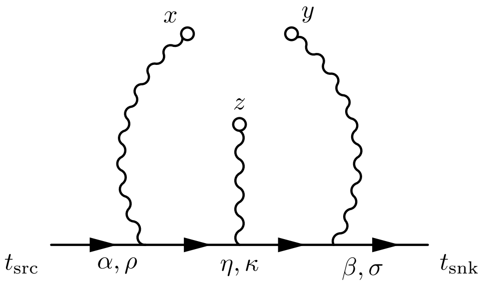


We define

$$i^3 \mathcal{G}_{\rho,\sigma,\kappa}(x,y,z) \quad = \quad \mathfrak{G}_{\rho,\sigma,\kappa}(x,y,z) + \mathfrak{G}_{\sigma,\kappa,\rho}(y,z,x) + \text{other 4 permutations}\,.$$

and add the Hermitian conjugate with permuted indices (does not alter $F_2$ but makes this kernel infrared finite)

$$\mathfrak{G}^{(1)}_{\rho,\sigma,\kappa}(x,y,z) \quad = \quad \frac{1}{2}\mathfrak{G}_{\rho,\sigma,\kappa}(x,y,z) + \frac{1}{2}[\mathfrak{G}_{\kappa,\sigma,\rho}(z,y,x)]^\dagger$$

For $m_{\rm line} = 1$ this yields the kernel

$$\begin{aligned}\mathfrak{G}^{(1)}_{\sigma,\kappa,\rho}(y,z,x) &= \frac{\gamma_0+1}{2} i\gamma_\sigma \left(-\,\overleftarrow{\partial\!\!\!/}_y + \gamma_0 + 1\right) i\gamma_\kappa \left(\,\overrightarrow{\partial\!\!\!/}_x + \gamma_0 + 1\right) i\gamma_\rho \frac{\gamma_0+1}{2} \\ &\quad \times \frac{1}{4\pi^2} \int d^4\eta \frac{1}{(\eta-z)^2} f(\eta-y) f(x-\eta).\end{aligned}$$

Due to current conservation, we can also devise a subtraction scheme that we found suppresses significantly finite-volume and discretization errors

$$\mathfrak{G}^{(2)}_{\rho,\sigma,\kappa}(x,y,z) = \mathfrak{G}^{(1)}_{\rho,\sigma,\kappa}(x,y,z) - \mathfrak{G}^{(1)}_{\rho,\sigma,\kappa}(y,y,z) - \mathfrak{G}^{(1)}_{\rho,\sigma,\kappa}(x,y,y) + \mathfrak{G}^{(1)}_{\rho,\sigma,\kappa}(y,y,y)$$

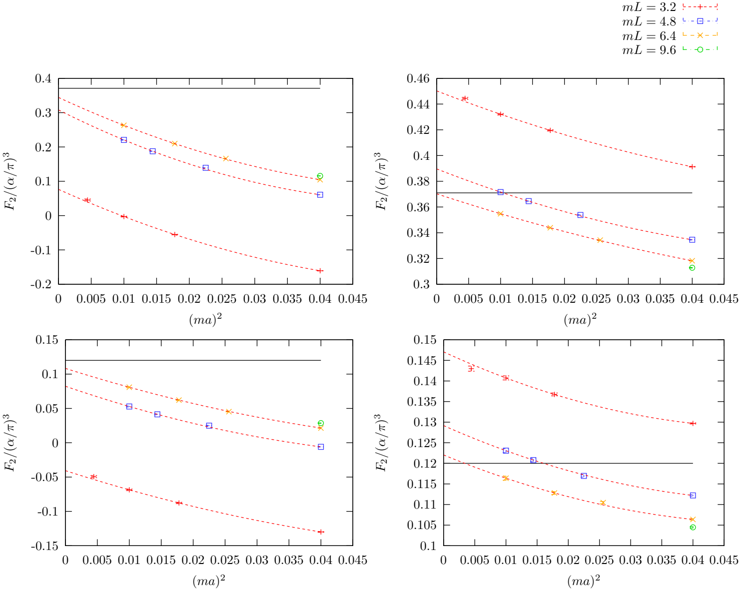


$m_{\rm loop} = m_{\rm line}$ (top), $m_{\rm loop} = 2m_{\rm lime}$ (bottom)
Without subtraction (left), with subtraction (right)

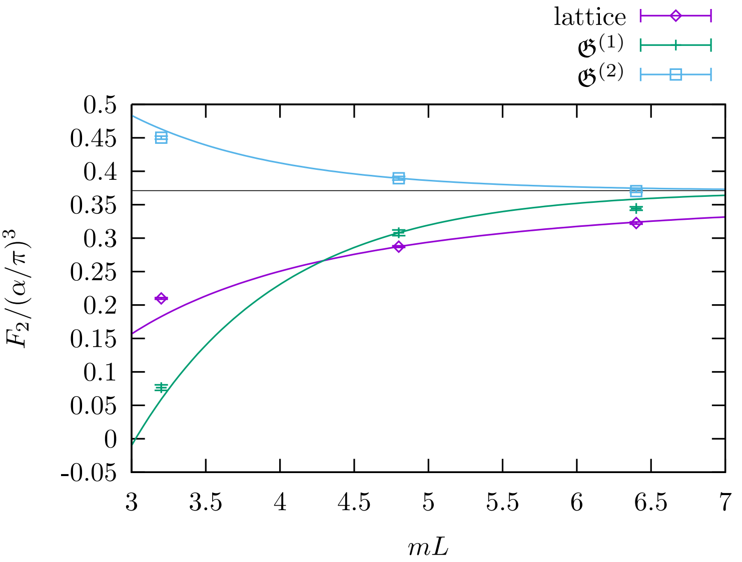


"Lattice" here refers to the previous finite-volume QED method

Preliminary combination of this infinite-volume kernel with lattice QCD data:

- QCD case with physical point quark mass,
- $48^3 \times 96$ lattice, with $a^{-1} = 1.73\,\mathrm{GeV}$, $m_\pi = 139\,\mathrm{MeV}$, $m_\mu = 106\,\mathrm{MeV}$.

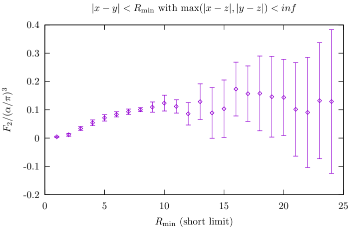


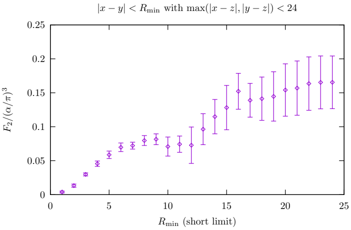


- c.f. QED$_L$ case, $\left.\frac{g_\mu - 2}{2}\right|_{\text{cHLbL}} = (0.0926 \pm 0.0077)\left(\frac{\alpha}{\pi}\right)^3$

Potentially large QCD FV effects (see also Andreas' talk): we are now starting measurements on a $(10\,fm)^3$ QCD box.

What is left to be done:

- Improve statistics of fine $64^3$ lattice run
- Improve statistics with infinite-volume QED kernel
- Complete run with infinite-volume QED kernel on $(10fm)^3$ QCD box

## Summary and outlook

New methods allow for a complete first-principles calculation of the hadronic light-by-light contribution to the $(g-2)_\mu$.

Control of all uncertainties on the 10% level over the next 1-2 years seems possible.

# Thank you

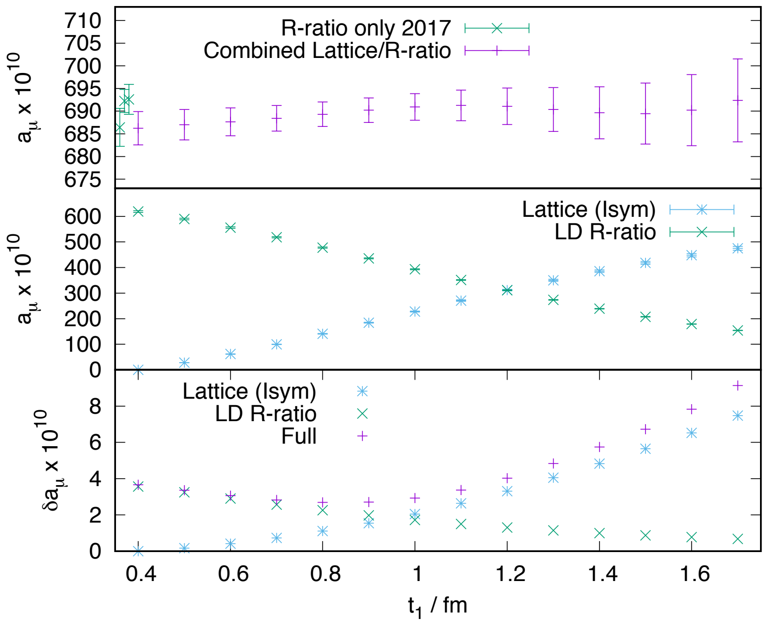

R-ratio only 2017
Combined Lattice/R-ratio
Lattice (Isym)
LD R-ratio
Full
$a_\mu \times 10^{10}$
$\delta a_\mu \times 10^{10}$
$t_1$ / fm

Low-mode saturation for physical pion mass (here 2000 modes):

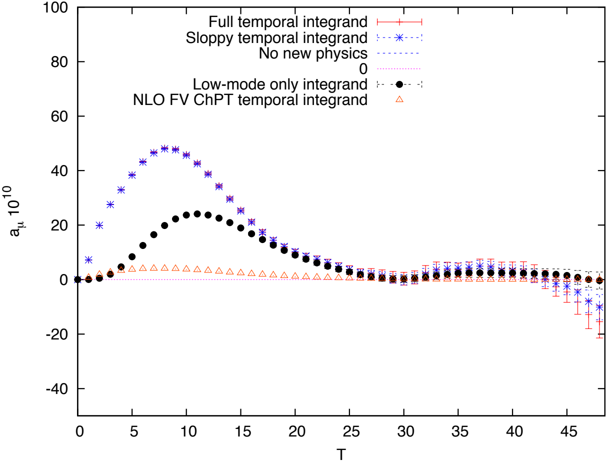

Result for partial sum $L_T = \sum_{t=0}^{T} w_t C(t)$:

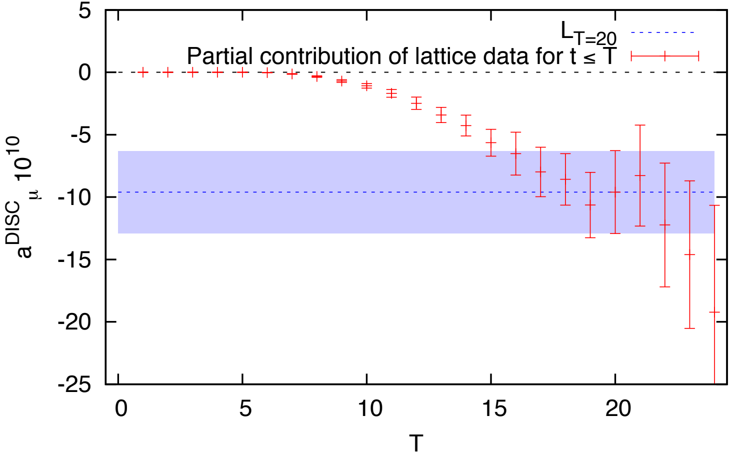


For $t \geq 15$ $C(t)$ is consistent with zero but the stochastic noise is $t$-independent and $w_t \propto t^4$ such that it is difficult to identify a plateau region based only on this plot

Resulting correlators and fit of $C(t) + C_s(t)$ to $c_\rho e^{-E_\rho t} + c_\phi e^{-E_\phi t}$ in the region $t \in [t_{\mathrm{min}}, \ldots, 17]$ with fixed energies $E_\rho = 770$ MeV and $E_\phi = 1020$. $C_s(t)$ is the strange connected correlator.

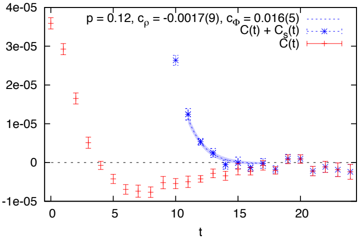


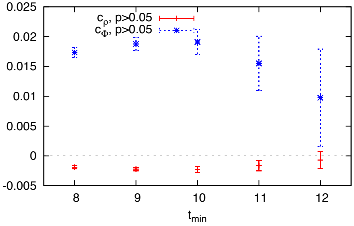


We fit to $C(t) + C_s(t)$ instead of $C(t)$ since the former has a spectral representation.

We could use this model alone for the long-distance tail to help identify a plateau but it would miss the two-pion tail

We therefore additionally calculate the two-pion tail for the disconnected diagram in ChPT:

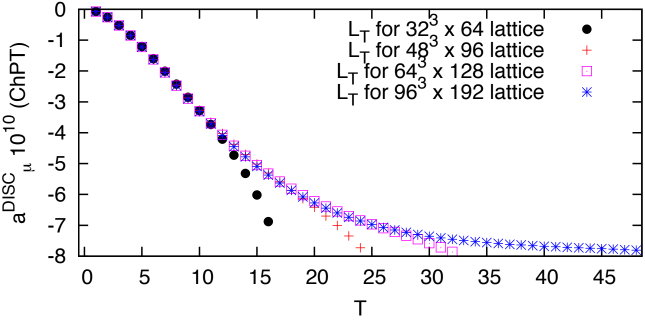

A closer look at the NLO FV ChPT prediction (1-loop sQED):

We show the partial sum $\sum_{t=0}^{T} w_t C(t)$ for different geometries and volumes:

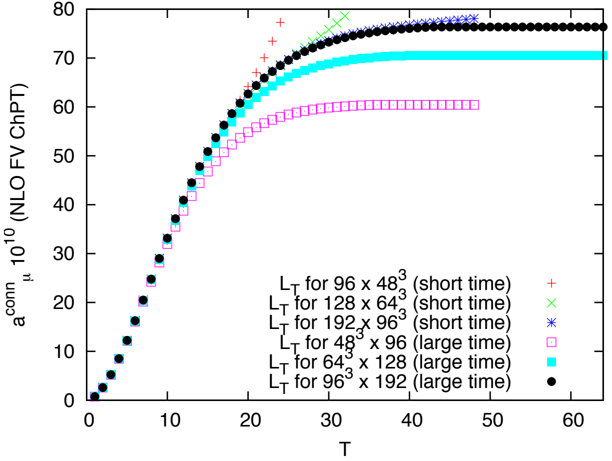

# The dispersive approach to HVP LO

The dispersion relation

$$\begin{aligned}\Pi_{\mu\nu}(q) &= i\left(q_\mu q_\nu - g_{\mu\nu} q^2\right)\Pi(q^2) \\ \Pi(q^2) &= -\frac{q^2}{\pi}\int_{4m_\pi^2}^{\infty}\frac{ds}{s}\frac{\mathrm{Im}\Pi(s)}{q^2-s}\,.\end{aligned}$$

allows for the determination of $a_\mu^{\mathrm{HVP}}$ from experimental data via

$$a_\mu^{\mathrm{HVP\ LO}} = \left(\frac{\alpha m_\mu}{3\pi}\right)^2\left[\int_{4m_\pi^2}^{E_0^2} ds\,\frac{R_\gamma^{\mathrm{exp}}(s)\hat{K}(s)}{s^2} + \int_{E_0^2}^{\infty} ds\,\frac{R_\gamma^{\mathrm{pQCD}}(s)\hat{K}(s)}{s^2}\right],$$

$$R_\gamma(s) = \sigma^{(0)}(e^+e^- \to \gamma^* \to \mathrm{hadrons})/\frac{4\pi\alpha^2}{3s}$$

Experimentally with or without additional hard photon (ISR: $e^+e^- \to \gamma^*(\to \mathrm{hadrons})\gamma$)

Experimental setup: muon storage ring with tuned momentum of muons to cancel leading coupling to electric field

$$\vec{\omega}_a = -\frac{q}{m}\left[a_\mu \vec{B} - \left(a_\mu - \frac{1}{\gamma^2 - 1}\right)\frac{\vec{\beta} \times \vec{E}}{c}\right]$$

Because of parity violation in weak decay of muon, a correlation between muon spin and decay electron direction exists, which can be used to measure the anomalous precession frequency $\omega_a$:

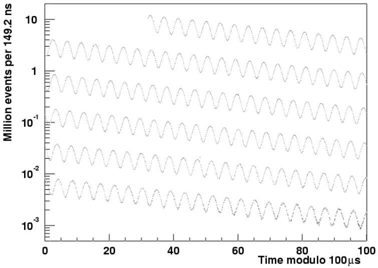

# BESIII 2015 update:

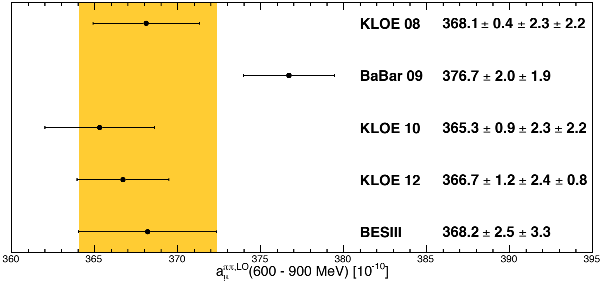

# Hagiwara et al. 2011:

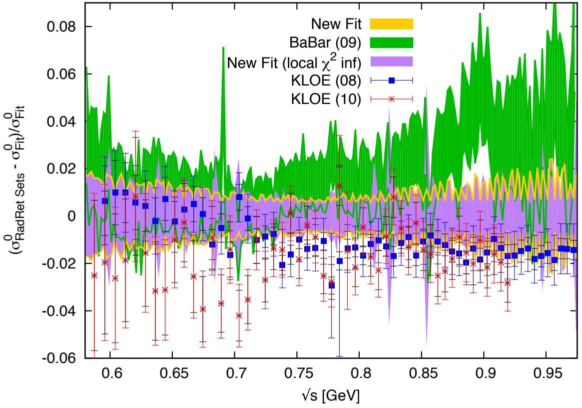

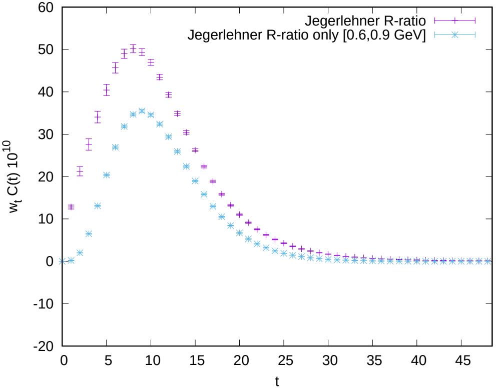


Problematic experimental region can readily be replaced by precise lattice data. Lattice also can be arbiter regarding different experimental data sets.

## Jegerlehner FCCP2015 summary:

| final state | range (GeV) | $a_\mu^{\text{had}(1)} \times 10^{10}$ (stat) (syst) [tot] | rel | abs |
|---|---|---|---|---|
| $\rho$ | ( 0.28, 1.05) | 507.55 ( 0.39) ( 2.68)[ 2.71] | 0.5% | 39.9% |
| $\omega$ | ( 0.42, 0.81) | 35.23 ( 0.42) ( 0.95)[ 1.04] | 3.0% | 5.9% |
| $\phi$ | ( 1.00, 1.04) | 34.31 ( 0.48) ( 0.79)[ 0.92] | 2.7% | 4.7% |
| $J/\psi$ | | 8.94 ( 0.42) ( 0.41)[ 0.59] | 6.6% | 1.9% |
| $\Upsilon$ | | 0.11 ( 0.00) ( 0.01)[ 0.01] | 6.8% | 0.0% |
| had | ( 1.05, 2.00) | 60.45 ( 0.21) ( 2.80)[ 2.80] | 4.6% | 42.9% |
| had | ( 2.00, 3.10) | 21.63 ( 0.12) ( 0.92)[ 0.93] | 4.3% | 4.7% |
| had | ( 3.10, 3.60) | 3.77 ( 0.03) ( 0.10)[ 0.10] | 2.8% | 0.1% |
| had | ( 3.60, 9.46) | 13.77 ( 0.04) ( 0.01)[ 0.04] | 0.3% | 0.0% |
| had | ( 9.46,13.00) | 1.28 ( 0.01) ( 0.07)[ 0.07] | 5.4% | 0.0% |
| pQCD | (13.0,$\infty$) | 1.53 ( 0.00) ( 0.00)[ 0.00] | 0.0% | 0.0% |
| data | ( 0.28,13.00) | 687.06 ( 0.89) ( 4.19)[ 4.28] | 0.6% | 0.0% |
| total | | 688.59 ( 0.89) ( 4.19)[ 4.28] | 0.6% | 100.0% |

Results for $a_\mu^{\text{had}(1)} \times 10^{10}$. Update August 2015, incl SCAN[NSK]+ISR[KLOE10,KLOE12,BaBar,BESIII]

# Jegerlehner FCCP2015 summary ($\tau \leftrightarrow e^+e^-$):

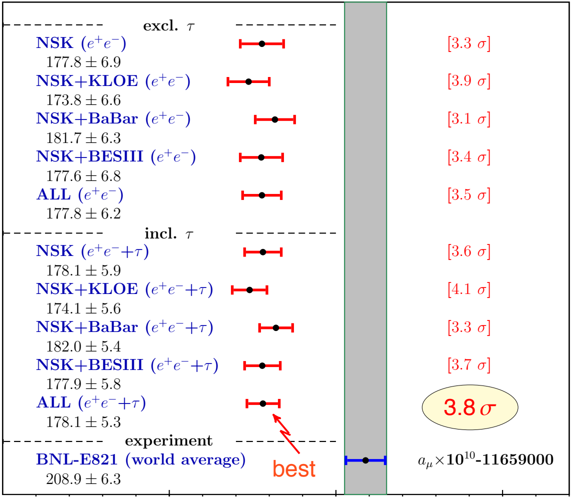

Our setup:

$$C(t) = \frac{1}{3V} \sum_{j=0,1,2} \sum_{t'} \langle \mathcal{V}_j(t+t') \mathcal{V}_j(t') \rangle_{\mathrm{SU(3)}} \tag{1}$$

where $V$ stands for the four-dimensional lattice volume, $\mathcal{V}_\mu = (1/3)(\mathcal{V}_\mu^{u/d} - \mathcal{V}_\mu^s)$, and

$$\mathcal{V}_\mu^f(t) = \sum_{\vec{x}} \mathrm{Im}\,\mathrm{Tr}[D^{-1}_{\vec{x},t;\vec{x},t}(m_f)\gamma_\mu] \,. \tag{2}$$

We separate 2000 low modes (up to around $m_s$) from light quark propagator as $D^{-1} = \sum_n v^n (w^n)^\dagger + D^{-1}_{\mathrm{high}}$ and estimate the high mode stochastically and the low modes as a full volume average Foley 2005.

We use a sparse grid for the high modes similar to Li 2010 which has support only for points $x_\mu$ with $(x_\mu - x_\mu^{(0)}) \bmod N = 0$; here we additionally use a random grid offset $x_\mu^{(0)}$ per sample allowing us to stochastically project to momenta.

Study $L_T = \sum_{t=T+1}^{\infty} w_t C(t)$ and use value of $T$ in plateau region (here $T = 20$) as central value. Use a combined estimate of a resonance model and the two-pion tail to estimate systematic uncertainty.

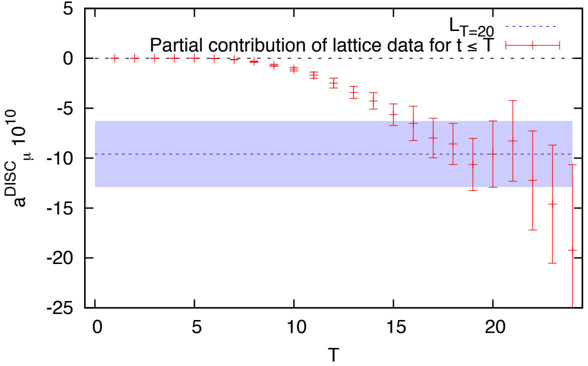


Combined with an estimate of discretization errors, we find

$$a_\mu^{\mathrm{HVP\ (LO)\ DISC}} = -9.6(3.3)_{\mathrm{stat}}(2.3)_{\mathrm{sys}} \times 10^{-10}\,. \tag{3}$$

# From Aubin et al. 2015 (arXiv:1512.07555v2)

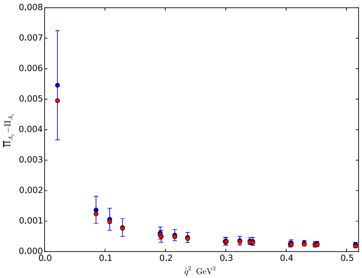


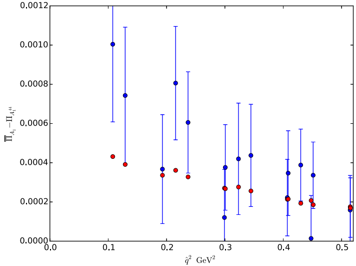


MILC lattice data with $m_\pi L = 4.2$, $m_\pi \approx 220$ MeV; Plot difference of $\Pi(q^2)$ from different irreps of 90-degree rotation symmetry of spatial components versus NLO FV ChPT prediction (red dots)

While the absolute value of $a_\mu$ is poorly described by the two-pion contribution, the volume dependence may be described sufficiently well to use ChPT to control FV errors at the 1% level; this needs further scrutiny

Aubin et al. find an $O(10\%)$ finite-volume error for $m_\pi L = 4.2$ based on the $A_1 - A_1^{44}$ difference (right-hand plot)

Compare difference of integrand of $48 \times 48 \times 96 \times 48$ (spatial) and $48 \times 48 \times 48 \times 96$ (temporal) geometries with NLO FV ChPT $(A_1 - A_1^{44})$:

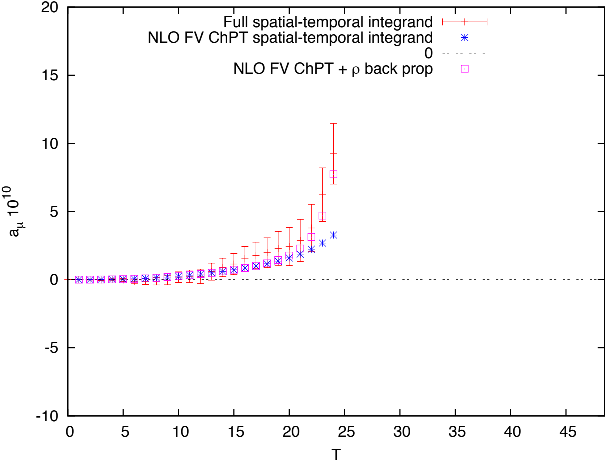


$m_\pi = 140$ MeV, $p^2 = m_\pi^2/(4\pi f_\pi)^2 \approx 0.7\%$

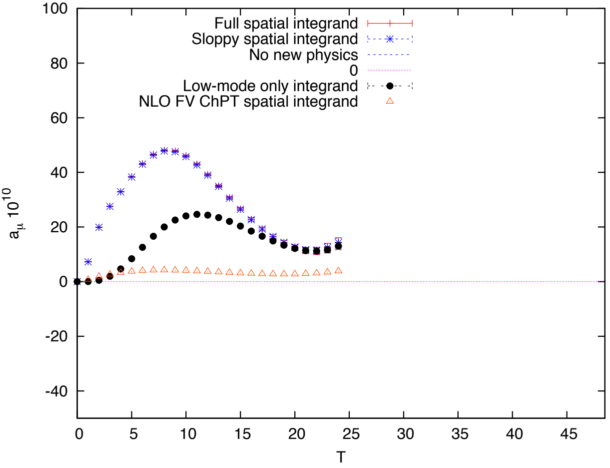

Full spatial integrand
Sloppy spatial integrand
No new physics
0
Low-mode only integrand
NLO FV ChPT spatial integrand
$a_\mu\ 10^{10}$
T
100
80
60
40
20
0
-20
-40
0
5
10
15
20
25
30
35
40
45